SCIENTIFIC CULTURE
www.sci-cult.com

SCIENTIFIC CULTURE, Vol. 6, No. 3, (2020), pp. 53-67
Open Access. Online & Print

DOI: 10.5281/zenodo.4007562

ARCHAEOLOGICAL GLASS CORROSION STUDIES: COMPOSITION, ENVIRONMENT AND CONTENT

Nikolaos Zacharias*[1], Eleni Palamara[1], Rania Kordali[1] and Vanessa Muros[1,2]

[1]Laboratory of Archaeometry, Department of History, Archaeology and Cultural Resources Management, University of the Peloponnese, Greece, Old Camp, 24133 Kalamata, Greece
[2]UCLA/Getty Conservation Program, A410 Fowler Building, Los Angeles, CA 90095-1510, U.S.A.

Received: 30/07/2020
Accepted: 02/09/2020

**Corresponding author: Nikolaos Zacharias (zacharias@uop.gr)*

ABSTRACT

Glass corrosion is a remarkably complex process, which can be affected by a wide range of diverse parameters, both external and internal, such as environmental conditions, glass composition, surface morphology, differences in manufacture, original content etc. The precise effect of these parameters still remains uncertain, despite the large number of studies focusing on the study of the corrosion mechanisms. The aim of the present study is to add in this academic discussion and specifically to highlight the complexity of corrosion phenomena and the effect of various parameters on the degradation of buried archaeological glass through the presentation of material from three case studies.

The examination of assemblages dated to different time periods from various sites throughout the country, from the North, Central and South Greece (Late Bronze Age glass from Pieria, Archaic to Hellenistic glass from Thebes, Roman glass from Patras and Ottoman glass from Kyparissia) highlights the influence of the burial environment and the complicate effect of glass composition and content in the corrosion process. Additionally, the above-mentioned case studies demonstrate the diversity of corrosion products and chemical/morphological patterns.

KEYWORDS: Glass corrosion, glass composition, vessel content, burial environment, corrosion products

1. INTRODUCTION

Glass is an intriguing material; it is relatively hard to make since it requires a specific mixture of several ingredients and a high firing temperature and it has been used in the past for the production of a plethora of everyday objects, as well as luxurious artefacts (Henderson 2013, Liritzis 2020). Corrosion of a glass object can be defined as the degradation or deterioration caused by external (e.g. environmental conditions) and/or internal factors (e.g. glass chemical composition) leading to a partial or complete loss of its functionality, (micro-) structure and/or shape (Melcher and Schreiner, 2013). The study of corrosion patterns provides vital information on the history, technology and use of the artefact (Zacharias and Palamara, 2016). The chemical processes associated with this deterioration are the result of the internal composition of the glass being attacked on a molecular level by external forces, principally involving water. The two primary mechanisms involved, namely de-alkalization, also referred to as leaching, and network dissolution, are described in detail elsewhere (Davison, 2003).

Glass corrosion can be affected by multiple parameters, the most important of which are the glass composition and the environmental conditions. Other parameters, such as surface morphology, differences in manufacture, original content of the vessel etc., can also play a very significant role in determining the mechanism and degree of glass corrosion (Melcher and Schreiner, 2013; Jackson et al., 2012; Palamara et al., 2016). The visual patterns of glass corrosion vary greatly and can include iridescence, dulling, spontaneous cracking, milky-like surface, black discolouration, Mn-browning and others (Davison, 2003).

Hench and Clark experimentally studied the likely chemical alterations appearing on the external surfaces of glass weathered in aqueous solution and ended in the description of six general types of possible permutations in the external glass surface (Hench, 1982; Hench and Clark, 1978; Hench et al., 1980). Out of these, the types more closely related to the corrosion of archaeological glass are types II, IV and V; in specific cases, type IIIA may also be applicable.

In the Type II surface, a silica-rich protective film is created, where the alkali has been lost but the silica network is not damaged. In the Type III surface a double protective surface film of aluminium silicate or calcium phosphate is formed; this type can exist in two versions, IIIA and IIIB. Glasses with Type II or Type IIIA surfaces appear undeteriorated, however the surfaces are largely leached of alkali. In the Type IV surface, a silica-rich film is again formed, but in this case the silica concentration is insufficient to protect the glass from migration of alkali or destruction of the network. The Type V surface is slowly soluble in the leaching solution. There is extensive loss of alkali accompanied by loss of silica, but because the attack on the glass is uniform, the surface composition remains the same as that of the bulk glass.

It should be highlighted, nevertheless, that glass corrosion remains a remarkably complex process, which can be affected by a wide range of diverse parameters and the precise effect of some parameters still remains uncertain (Davison, 2003). As Harden emphatically stated: "...it is quite impossible to foresee what type or degree of weathering will be produced on a piece of glass after preservation for a fixed time under seemingly fixed circumstances ... even a very slight change in environment may produce a markedly different kind or degree of weathering on two parts of the same vessel ... No strict rules can therefore be formulated. The causes and effects of weathering are as manifold as they are elusive" (Harden, 1936).

The study of corrosion mechanisms and durability of glass started as early as the mid 17th c. (Melcher and Schreiner, 2013). In the mid 20th c. more emphasis was given in these studies, in an effort to take advantage of the lack of chemical activity of glass in order to use glass vessels for the storage of radioactive waste (representative bibliography provided by Verney-Carron (2017)). The most recent corrosion studies of archaeological and historical glass combine multiple diverse microscopic and analytic techniques, aiming to achieve a holistic overview of the underlying corrosion phenomena as well the best suited conservation approaches. So far, more emphasis has been given to the corrosion study of European medieval glass panes, whereas the corrosion of archaeological glass buried in the ground has not received a lot of attention (Pollard and Heron, 1996). Some indicative examples are the investigation of the environmental effect in the corrosion processes of Italian archaeological glass (Silvestri et al., 2005), the corrosion and conservation study of archaeological glass from Spain (Doménech-Carbó et al., 2006) and historical glass panes from Britain (Cagno et al., 2011), the study of Mn-browning in historical glass panes from Belgium (Schalm et al., 2011), and the investigation of the corrosion of archaeological glass buried in acidic environment (Jackson et al., 2012).

The aim of the present study is to add in this academic discussion and specifically to highlight the complexity of corrosion phenomena and the effect of various parameters on the degradation of buried archaeological glass through the presentation of material from three case studies. The examination of

two assemblages of Ottoman and Roman glasses highlights the effect of glass composition and content, respectively, in the corrosion process. Additionally, the study of Late Bronze Age glass demonstrates the effect of the burial environment and the complexity of corrosion products.

2. METHODOLOGY

Optical microscopy using a fibre optics system (FOM/i-scope, Moritex) was performed on all samples aiming at the detailed documentation of the complex visual corrosion patterns. The chemical analysis of the samples was carried out using a Scanning Electron Microscopy, type JEOL JSM–6510LV, coupled with an Oxford Instruments Energy Dispersive Spectrometer. The analytical data were obtained by INKA software. Analyses were conducted at high vacuum, 20 kV accelerating voltage and with a count time varying between 100 and 300 sec. Detailed information on the precision and accuracy of the device is provided by Palamara et al. (2016).

3. CORROSION AND GLASS COMPOSITION

The assemblage studied here was recovered in a small Ottoman public bathhouse (hamam) in Kyparissia, southern Greece. The structure was revealed when a house, built on top of the remaining parts of the bathhouse, was demolished. The restoration work was limited to the debris removal and to the excavation of the main parts of the bathhouse without expanding to the rest of the building. The exact time of construction is unknown. However, a bathhouse was mentioned by the Ottoman traveler Evliyâ Çelebi at 1668; assuming that his testimony is a reference to this bathhouse, we have a date that serves as a terminus ante quem. Certain aspects of the building (e.g. its simplified construction, the lack of decorated internal surfaces and the extended use of bricks), in conjunction with the recovered pottery, suggest that the hammam was likely constructed around the first half of the 17th c. (Germanidou and Gerolymou, 2015).

A number of glass sherds were recovered from the bathhouse; 42 samples were selected for microscopic examination and chemical analysis using SEM/EDS (Palamara et al., 2017). All samples are from small vessels or tableware; the majority are colourless, or colourless with a slight yellow, pink or grey tinge. The coloured samples have a green (1), light blue (3) and blue hue (2). All the items have thick walls and demonstrate almost no decorative patterns.

The chemical analysis of the samples showed significant variability for all major elements, suggesting the simultaneous presence of many different glass types. Following the categorization by Dungworth et al. (2006) for medieval and post-medieval glass, we can divide the samples of the assemblage into 4 distinct groups of glass and one outlier (Table 1):

• Group I: Comprises of 3 K-rich glasses. All samples are clear and colourless. They are characterized by very low Al_2O_3 levels (<0.25 wt%), but their CaO concentration varies significantly (between 5.5 and 8 wt%). The very low magnesium and phosphorus concentration of the samples suggests that the potassium source is saltpetre or potash, instead of K-rich plant-ash. The lack of a green tinge also suggests that this group does not belong to the forest glass type, but is either crystal or chalk glass.

• Group II: Comprises of 4 mixed alkali glasses. All the samples of this group are colourless or naturally coloured with a yellow tinge. The variability of all major oxides is high in this group. The samples have characteristically high silica concentration (>77 wt %), calcium values vary between 4.6 and 7 wt% and the Na_2O/K_2O ratio varies between 1.1 and 1.7.

• Group III: Comprises of 28 Na-rich glasses. The majority of the samples are colourless or naturally coloured with a yellow, pink or grey tinge. The group also includes three light blue and one dark blue sample. Three samples with low-lead concentration also belong to this group. The alkali source for this group is plant-ash rich in sodium. The concentration of the major elements presents high variability within this group. Apart from the difference in raw materials and recipes used, the observed compositional heterogeneity could also be the result of recycling. The samples of this group could be further divided into 6 sub-groups and 4 outliers.

• Group IV: Comprises of 6 Na-rich glasses. The silica source in this groups is again plant-ash rich in sodium. Four samples are colourless or naturally coloured with a green tinge. The other samples show green and dark blue colours. The composition of Na_2O, K_2O and MgO is similar to that of Group III samples. However, the samples of this group demonstrate a characteristically high and homogeneous concentration of calcium (approximately 11 wt%). The concentration of alumina is elevated compared to the other samples of the assemblage, but varies greatly from 0.5 to 2.5 wt%.

• High-Pb glass: Sample 219-4 is distinguished by its high concentration in lead (23 wt%). The sample is colourless and clear, and does not present any decorative patterns. The primary alkali is potassium, although sodium is also present in relatively high concentration. As expected for lead glasses, the concentration of all other oxides is very low (<0.4 wt%).

Table 1. Mean value (μ) and standard deviation (s) for the concentration (in wt%) of the major oxides for each group and sub-group of the assemblage.

Group	No. of samples		Na_2O	MgO	Al_2O_3	SiO_2	P_2O_5	K_2O	CaO	TiO_2	MnO	FeO	CuO	PbO
I	3	μ	1.27	0.98	0.11	76.65	0.14	13.77	6.92	0.08	nd	0.09	nd	nd
		s	0.50	0.62	0.08	1.12	0.04	0.34	1.26	0.02	-	0.03	-	-
II	4	μ	8.63	0.30	0.13	78.02	0.11	6.57	5.92	0.02	0.19	0.10	nd	nd
		s	1.82	0.22	0.09	0.58	0.08	0.38	1.24	0.03	0.21	0.08	-	-
IIIa	7	μ	16.63	0.33	0.24	76.07	0.05	0.95	5.25	0.06	0.11	0.07	0.25	nd
		s	1.38	0.06	0.06	1.42	0.07	0.20	0.38	0.05	0.07	0.06	0.32	-
IIIb	6	μ	16.75	0.65	0.30	75.86	0.02	0.38	5.79	0.04	0.09	0.12	0.02	nd
		s	2.11	0.47	0.14	2.85	0.02	0.05	0.57	0.05	0.07	0.04	0.04	-
IIIc	4	μ	13.21	0.49	0.21	76.83	0.14	4.40	4.63	0.02	0.03	0.04	nd	nd
		s	0.87	0.34	0.10	1.07	0.08	0.22	0.56	0.02	0.06	0.05	-	-
IIId	2	μ	15.65	1.86	1.06	71.62	0.45	3.14	5.64	nd	0.29	0.29	nd	nd
		s	0.54	0.03	0.15	0.08	0.04	0.15	0.51	-	0.03	0.05	-	-
IIIe	2	μ	15.07	0.15	0.09	77.61	0.02	0.51	6.37	0.12	0.04	0.03	nd	nd
			0.88	0.02	0.06	0.32	0.02	0.00	0.59	0.11	0.06	0.05	-	-
III+Pb	3	μ	15.42	0.57	0.31	74.32	0.01	1.16	5.70	0.05	0.12	0.05	nd	2.30
		s	0.93	0.03	0.03	1.53	0.01	0.51	0.21	0.06	0.02	0.04	-	0.24
Outlier 1	1		17.53	0.11	0.05	74.53	0.07	0.03	7.60	0.09	nd	nd	nd	nd
Outlier 2	1		17.35	0.55	0.65	73.77	0.00	0.17	7.34	nd	nd	0.16	nd	nd
Outlier 3	1		15.93	0.07	0.26	75.41	0.05	0.12	7.90	0.04	0.22	nd	nd	nd
Outlier 4	1		19.99	4.71	1.59	65.89	0.28	1.62	5.35	0.06	0.30	0.22	nd	nd
IV	6	μ	14.51	0.48	1.42	72.30	0.03	0.42	10.37	0.10	0.18	0.19	nd	nd
		s	0.68	0.16	0.62	0.91	0.07	0.24	0.67	0.06	0.18	0.10	-	-
Pb	1		2.51	0.25	0.29	64.51	0.26	8.65	0.37	0.12	nd	nd	nd	23.06

The vast chemical heterogeneity of the samples, which were all recovered from the same location, make this assemblage a perfect case study for the effect of composition in the corrosion of glass. Based on the macroscopic and microscopic examination, the glass sherds do not present significant signs of corrosion. Most samples present iridescence, dulling and/or milky-like surfaces. A few samples additionally present pitting (Fig. 1).

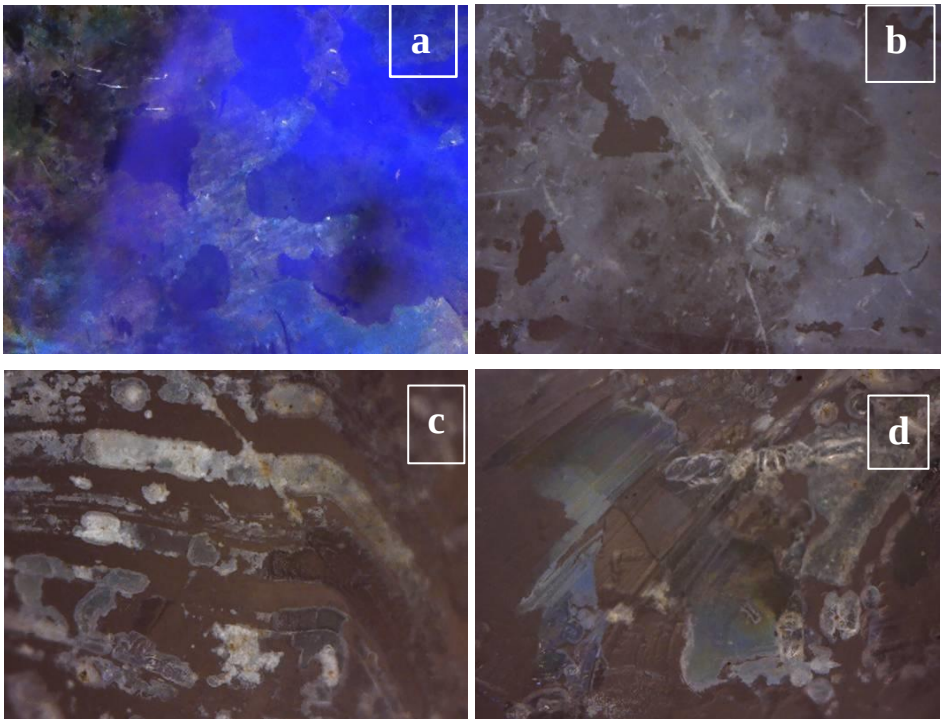

Figure 1. Representative LED images (magnification x50) from surfaces showing iridescence (a), dulling (b), milky-like surface (c) and pitting (d)

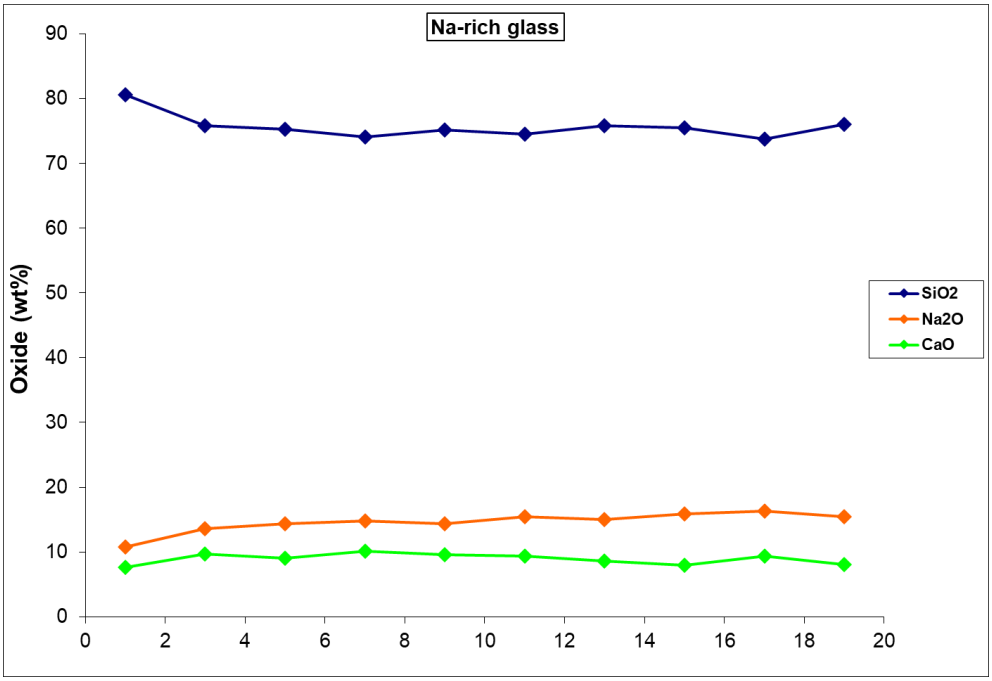
Na-rich glass
Oxide (wt%)
SiO2
Na2O
CaO

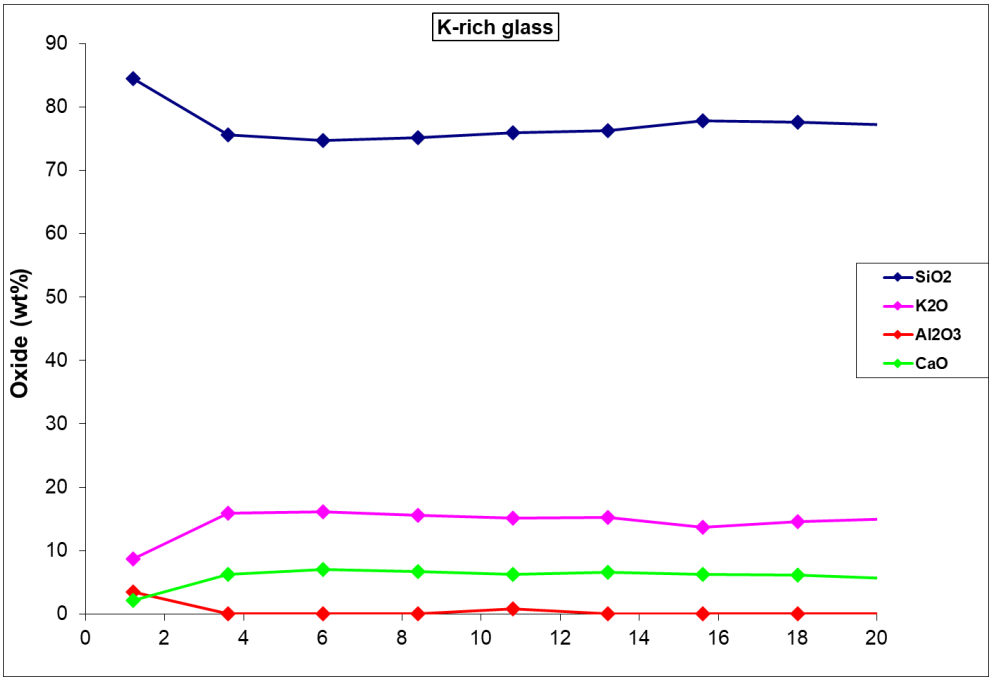
K-rich glass
Oxide (wt%)
SiO2
K2O
Al2O3
CaO

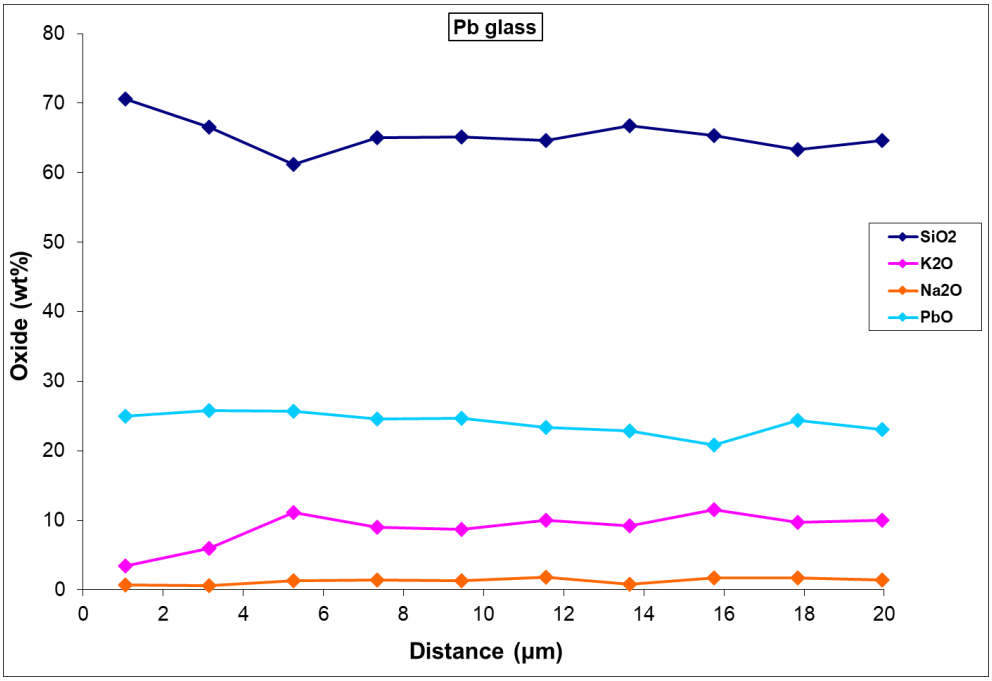

Figure 2. Representative concentration profiles of the main oxides, as determined by SEM/EDS, for K-rich glasses (up), Na-rich glass (middle) and high-lead glass (down) (0 μm: external surface).

The degree and the mechanism of corrosion for each sample was further investigated by conducting chemical analyses using a SEM/EDS along cross sections of fresh cuts. Figure 2 shows the representative concentration profiles for the Na-rich, the K-rich and the high-lead group, focusing at a layer of 20 μm in the external sherd surface; in all cases the analyzed samples were colourless.

Based on the concntration profiles, the chemical alteration of the external surfaces is limited; a thin layer of 3-6 μm is usually present. The Na-rich glass presents the smallest degree of corrosion, with a small decrease in the concentration of Na2O and a respective increase in SiO_2, in an external layer of 3 μm. Calcium content remains stable along the cross section, whereas the composition of Al_2O_3 was too low to evaluate likely changes. Overall, the chemical profile resembles a Type II surface, based on the categorization of corroded glass surfaces by Hench (1982), which was mentioned before.

K-rich glass presents stronger corrosion, with a significant decrease in the concentration of K_2O and CaO, and a resulting increase in SiO_2. The amount of Al_2O_3 is additionally increased significantly, suggesting the formation of an external Al_2O_3-SiO_2 protective layer, and therefore a Type III corrosion layer. It is has been suggested in literature that K-rich glasses present different mechanisms and higher rates of corrosion compared to Na-rich glasses (Bertoncello et al., 2002; Domenech-Carbo et al., 2006, Tournie et al., 2008). The present results further support this theory.

Finally, the high-lead glass presents the thickest external layer of corrosion, with a width of 6 μm; in this layer, K2O is decreased by half and SiO_2 is increased. The concentration of lead remains stable throughout the cross section.

4. CORROSION AND VESSEL CONTENT

During a systematic excavation of a Roman funerary complex (2nd c. AD) at the city of Patras, Achaia, an assemblage of luxurious glass vessels was recovered, found placed together in a wooden chest. Some of the items are considered to be unique amongst Roman products found in the Aegean. The vessels have a wide variety of colours, from transparent colourless to translucent blue, green and purple, but here we will focus only on the colourless samples of the assemblage.

The chemical composition of the samples was determined using SEM-EDS (Table 2). All colourless samples belong to the general type of soda-lime-silica glass and have a typical concentration for colourless Roman glass of the 2nd-3rd c. AD (Freestone et al., 2002). The alkali source used is natron and a combination of both antimonate and manganese is introduced as decolourisers.

Table 2. SEM/EDS compositional analysis of the body of colourless vessel fragments (weight %, normalised to 100%)

	Na_2O	MgO	Al_2O_3	SiO_2	SO_3	Cl	K_2O	CaO	TiO_2	MnO	FeO	Sb_2O_3
Mean	19.54	0.42	2.42	68.94	0.25	1.00	0.34	6.15	0.19	0.50	0.24	0.79
s	0.50	0.19	0.25	0.79	0.19	0.11	0.10	0.25	0.14	0.18	0.14	0.49

A residue of an intense pink colour was found attached to the inner surface of a number of the colourless samples (Figure 3). The chemical analysis of the residue showed that it is an aluminosilicate substance, with a relatively high sulphur content (Table 3). Both the colour of the residue and its chemical composition resemble madder lake, a red lake pigment which was used during the Roman period (Eastaugh et al., 2004). The pigment is extracted from the common madder plant Rubia tinctorum and can contain two organic red dyes: alizarin and purpurin. Since madder lake is in the form of a very fine powder and has very little bulk it must be precipitated on an inert pigment or lake base, in order to make it suitable for brushing. Clay or alum was often used for this purpose.

***Table 3. SEM/*EDS compositional analysis of the pink residue (weight %, normalised to 100%)**

	MgO	**Al_2O_3**	**SiO_2**	**SO_3**	**K_2O**	CaO	**TiO_2**	**FeO**
Mean	2.23	45.34	41.74	2.66	1.34	2.64	0.38	3.68
s	0.08	0.92	0.31	0.22	0.20	0.06	0.20	0.30

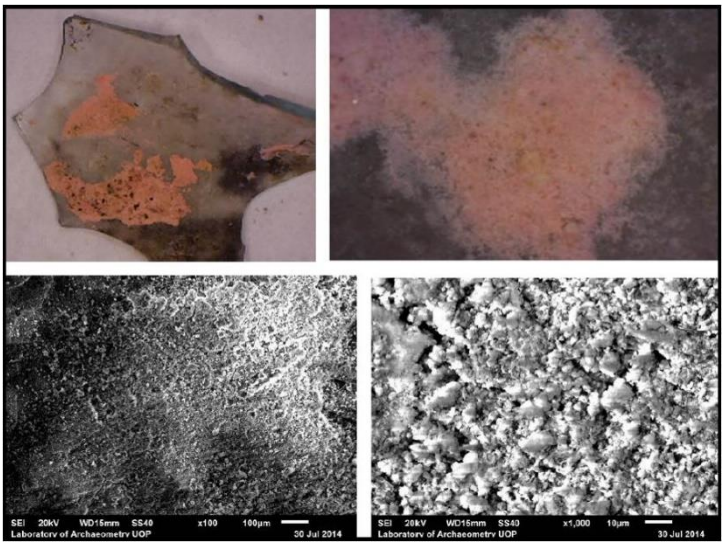

Figure 3. LED microscope (Left: x10; Right: x50) and SEM images (Left: x100; Right: x1000) of the pink residue.

In order to securely identify the residue, the spectrometric technique of Laser Desorption –Ionization – Time of Flight – Mass Spectrometry (LDI-ToF-MS) was applied. The analysis securely identified the presence of alizarin as the main component of the organic extract and therefore verified the characterization of the pink residue as a madder lake.

The presence of the aluminosilicate residue has resulted in the extensive corrosion of the inside surface of the vessels. In fact, the inner surface seems significantly more corroded than the outer one, which was not in direct contact with the madder lake as long as the vessels remained intact.

Figure 4 shows a concentration profile of the major elements conducted on a fresh section of a colourless sample, focusing specifically on two zones of 40 µm on the inside and outside edge of the vessel's wall. In both cases, a layer is formed which shows a high loss of alkali and a consequent increase in the concentration of silica and alumina. On the inner corrosion zone, an increase in calcium is also noted. However, the external corrosion layer seems to be very thin, approximately 2 µm in depth, while the inner corrosion layer has a depth of over 15 µm. We suggest, therefore, that the original content played a critical role in the corrosion effects of the glass samples, even in cases where the vessels broke at some unknown point in the past.

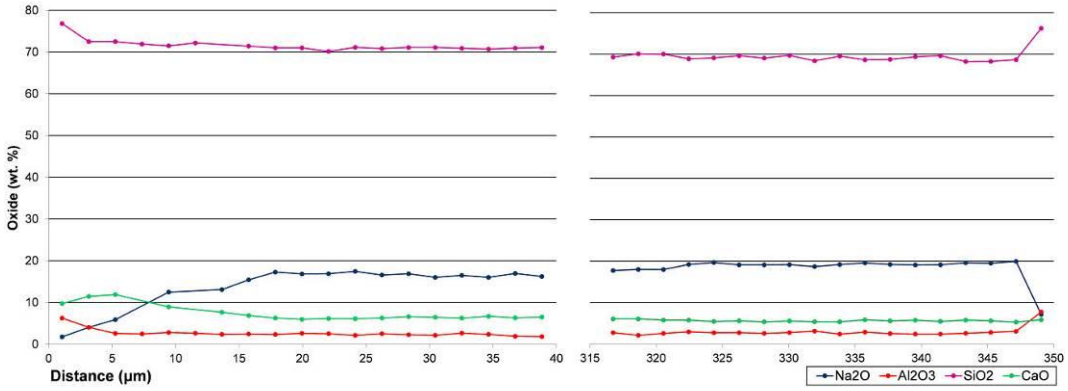

Figure 4. Concentration profile by SEM/EDS (0 μm: Inner surface; 350 μm: Outer surface).

Another corrosion alteration which is likely to be associated with the madder lake residue is the formation of areas that show high iridescence and have a flaky appearance under the SEM (Figure 5). The formation of iridescent areas is common in weathered glass (Davison, 2003). However, certain aspects of the formations under examination are of particular interest. The iridescent layers are only present in the inner surfaces of the colourless samples and did not flake away during the process of cleaning. Moreover, they appear in well-formed stripes with areas of clear glass between them. The chemical composition of both the clear and the iridescent areas is characterized by an almost complete loss of alkalis and, to a smaller degree, of calcium, and a consequent increase in the concentration of silica and alumina (Table 4). However, the iridescent areas have a twice as high concentration of aluminium, suggesting precipitation of alumina from the surrounding. The exact way the iridescent stripes were formed and the likely connection with the madder lake residue is still under investigation.

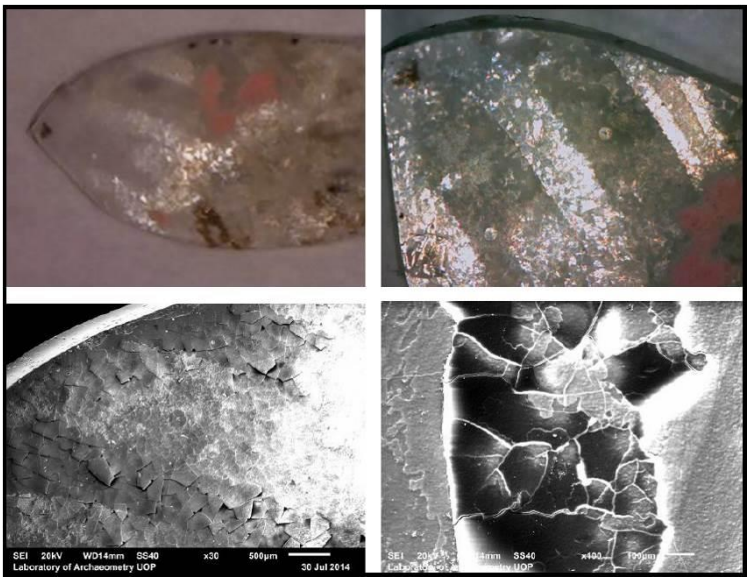

Figure 5. LED microscope (Left: x10; Right: x50) and SEM images (Left: x30; Right: x100) of iridescent layers on the inner surface of colourless fragments.

Table 4. SEM/EDS compositional analysis of clear and iridescent surfaces on the colourless vessel fragments (weight %, normalised to 100%)

	Na_2O	MgO	Al_2O_3	SiO_2	SO_3	Cl	K_2O	CaO	TiO_2	MnO	FeO	Sb_2O_3
Clear	0.25	0.57	4.86	86.25	0.28	0.52	0.22	5.77	0.05	0.56	0.28	0.39
Iridescent	0.59	0.58	9.56	81.55	0.52	0.42	0.28	4.99	0.08	0.43	0.35	0.64

5. CORROSION AND BURIAL ENVIRONMENT

As described previously, the burial environment has a great influence on the preservation of archaeological glass and the levels and types of deterioration observed. Factors such as moisture levels, soil pH, migration of ions and microorganism all play a major role in the appearance and composition of glass when excavated (Freestone 2001). This in turn can have an effect on research conducted on ancient glass technologies since corrosion can affect the composition of the glass or it can result in the loss of material to be studied which can create gaps in the knowledge around glass technology, manufacture and trade.

A case study that highlights some of the typical corrosion and surface morphologies of deteriorated archaeological glass are seen in the Late Bronze Age beads excavated at the site of Ancient Methone in northern Greece. The beads were excavated between 2005-2010 by archaeologists from the Ephorate of Antiquities in Pieria and found within four burials from the Late Bronze Age cemetery (14th-13th c. BCE). 47 glass beads were discovered and most of these were in very poor condition. The glass beads were severely corroded and had become opaque, ranging in color from white to yellow to yellow-brown. Many of these beads were fragile and had little to no intact glass remaining in the core. For those beads that did have intact glass visible, the glass appeared iridescent and the surface was pitted. Staining was present on the exterior of many of the beads. The stains were mainly black or dark brown in color and ranged in appearance from spots to linear or circular forms.

The deterioration of glass in the soil can occur due to an ion exchange mechanism and the dissolution of silica. Both can occur at the same time but the ion exchange deterioration mechanism is the more likely cause of glass weathering and corrosion (Freestone, 2001). This creates a glass surface layer that is depleted in alkali and alkali earth elements and enriched in silica which can appear iridescent or opaque. The corrosion layers form tend to be layered or laminar and have been observed to have certain types of morphologies such as a zigzag, parallel or hemispherical structures (Cox and Ford, 1993; Doménech-Carbó et al., 2006). Some of these morphologies were observed on the Ancient Methone beads (Figure 6). The thickness of this layer depends on the composition of the glass and the burial environment, as well as how long the object has been buried. Glasses that are heavily corroded can become completely opaque and could lose their structure becoming flaky or losing all cohesion and becoming extremely fragile and fragmentary. Several of the beads studied also exhibited a flaky and opaque surface.

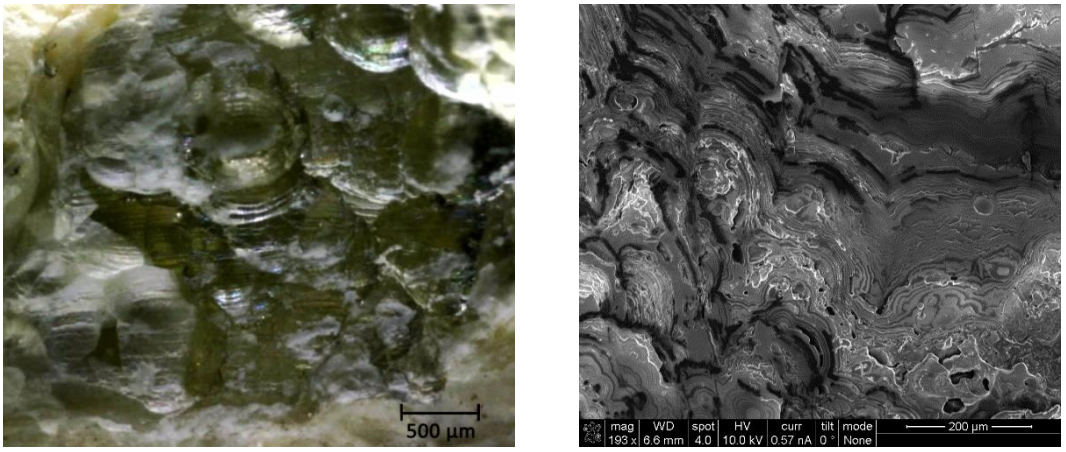

Figure 6. Left: Photomicrograph of the surface of glass bead MEΘ 4164-1 from Tomb 245/5 showing macropitting and a surface damage in the form of hemispherical and parallel lines. Right: SEM image taken of the surface of glass bead MEΘ 890-2, also from Tomb 245/5, showing laminar corrosion layers.

The loss of alkali and alkali earth components during glass corrosion leaves a glass depleted in soda, potash and to some extent magnesia (Cox and Ford, 1993; Doménech-Carbó et al., 2006; Perez y Jorba et al., 1980). These areas become enriched in elements that are not as soluble, such as silica and alumina. Other elements tend to be found in higher concentrations as well, namely manganese and iron oxides. Some examples were also found with higher concentrations of Pb, Sn and Sb (Doménech-Carbó et al., 2006; Freestone, 2001; Palamara et al., 2016). The enriched elements do not necessarily have to be found within the glass core but can be found on the surface, as with elements such as Mn and Fe. It is possible that this is caused by the solubilization of these components within the glass that then get precipitated onto the surface (Doménech-Carbó et al., 2006). These elements entering the glass matrix from

the burial environment is also a possibility. Due the effect of this deterioration, analytical techniques which only analyze the surface of a sample will not provide a true representation of the composition of the glass, even if the area targeted appears to be intact glass or only slightly deteriorated. This is evident from SEM-EDS analysis conducted on a group of beads from Ancient Methone (Table 5). Most have little to no Na_2O remaining and K_2O and MgO concentrations are low in several of the beads. Enrichment of Al_2O, MnO and FeO on the surface of the majority of the Ancient Methone beads was found.

Table 5. Composition of a group of deteriorated Ancient Methone beads analyzed with SEM-EDS. All values given as wt. oxide % and normalized to 100%.

Bead No.	Na_2O	MgO	Al_2O_3	SiO_2	P_2O_5	SO_3	K_2O	CaO	TiO_2	MnO	FeO	CoO	CuO	PbO
Yellow/yellow-green/green														
889-2	0.77	4.90	2.56	83.00	n.d	0.37	1.57	4.04	0.79	n.d	1.11	n.d	0.90	n.d
889-3	nd	2.03	2.90	86.05	nd	1.29	0.73	3.71	nd	nd	3.29	nd	nd	nd
889-4	nd	1.11	2.66	87.82	nd	0.62	0.49	1.92	nd	nd	5.38	nd	nd	nd
889-5	12.39	4.58	2.40	67.81	nd	1.25	2.13	4.13	nd	nd	2.32	nd	nd	2.99
889-6	18.52	6.02	1.57	61.13	nd	1.02	3.17	4.65	nd	0.56	1.52	nd	0.61	1.22
889-7	nd	1.52	5.64	84.70	nd	0.13	0.47	2.38	nd	nd	2.68	nd	1.37	1.12
890-1	1.14	3.14	4.55	75.90	1.14	1.17	1.84	7.31	nd	nd	3.81	nd	nd	nd
890-3	2.57	1.95	5.40	77.39	nd	0.92	0.86	4.64	nd	nd	6.28	nd	nd	nd
890-4	nd	2.20	5.93	80.82	nd	nd	1.01	3.88	nd	0.76	5.40	nd	nd	nd
890-5	0.62	2.03	4.71	83.75	nd	nd	0.63	3.27	nd	nd	3.26	nd	nd	1.73
4164-1	1.92	1.85	4.28	80.98	n.d	0.95	0.61	3.47	n.d	n.d	3.70	n.d	n.d	2.24
Dark green														
884β	nd	1.33	3.84	64.17	nd	nd	0.42	3.50	nd	nd	2.97	nd	23.78	nd
Black/dark gray														
889-8	nd	1.97	1.73	88.17	nd	1.32	0.36	4.19	nd	2.26	nd	nd	nd	nd
nd= element not detected														

Microorganisms can also play a role in the deterioration of glass. Biocorrosion can result in darkening of glass, as spots or rings or physical damage represented by very circular holes or groups of concentric circles (Palamara et al., 2016; Perez y Jorba et al., 1980) (Fig. 7). The activity of bacteria can also leave areas enriched in elements such as Mn, Fe and S. In the case of the Ancient Methone beads, dark rings, semi-circular and linear black bands were found on many of the opaque glass beads. The enrichment of Mn and Fe on the surface of the glass beads has already been discussed in the previous sections. SO_3 was found on the surface of 11 of the 14 beads analyzed using EDS. Sulfur has been found within the raw materials used for glass, such as in the plant ash used for the flux in LBA glasses, and can be present in concentrations up to 0.3% (as SO_3). The concentrations of SO_3 in the Ancient Methone beads in the areas analyzed range from 0.03-0.35% and fall within that range so it is difficult to determine whether its presence is due to the plant ash used or the action of microorganisms.

Figure 7. Left: The surface of glass bead MEΘ 889-3 (Tomb 245/5) shows deterioration likely caused by microorganisms, in the form of groups of concentric circles and dark bands. Right: SEM images taken of the surface of bead MEΘ 884β shows evidence of deterioration due to microorganisms as both groups of concentric circles and circular holes.

6. CORROSION PATTERNS AND SURFACE MORPHOLOGY

In this case study, an assemblage of glass samples with different morphological characteristics has been analysed with state of the art analytical techniques. The collection consists of 16 coloured glass fragments, 13 beads and 3 core-formed vessels. The assemblage originates from mainland Greece, Thebes from two different excavation sites. The beads recovered from an ancient cemetery, discovered during the construction of a bridge at the outskirts of Thebes and the core formed vessels been recovered from a systematic excavation at the center of the city. The dating range of the fragments varies from Archaic to Hellenistic period. The beads have a variety of coloration such as green, white, light and dark blue, brown, black, and colorless with blueish hue, while the vessel fragments have deep blue color with yellow and white trail decoration characteristic of the core-formed technique.

This work aims to identify the chemical composition and the degree of the alkali loss, to determine the corrosion patterns occurred, and to examine the degree of corrosion in glass with different surface finishes. The examination was performed in three different manufacturing surfaces: even craft surface (beads), uneven surface (2 colored beads-fused surface), and uneven surface, valleys-ridges (vessels - decoration trails).

Different corrosion patterns identified under the examination with LED-OM, iridescence was the most common. The majority of the samples occurred pitting and micro-pitting, with pits and craters filled with thin glass layers. The semi opaque milky enamel like effect observed at the colourless samples and dark brown and black staining at the white beads. Concentric layers forming local crust, lamination and flaking that were observed to create geometrical formations in the surface of the samples. The lamination layers observed to have different thicknesses and sizes. (Cox and Ford, 1993; Doménech-Carbó et al., 2006; Rahman et al., 2019). (Fig 8).

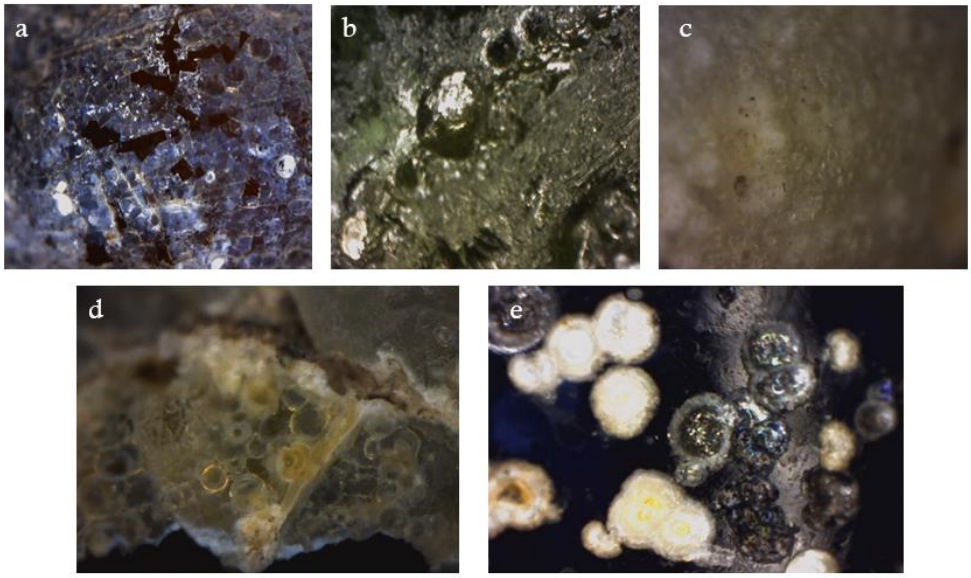

Figure 8. Identified corrosion patterns under LED-OM: a (up left) iridescence, b (up centre) pitting, c (up right) dark brown and black staining in white sample, d (down left) semi opaque milky like surface and e (down right) pitting with characteristic concentric layers forming local crust.

Chemical analysis performed by SEM/EDS for major and minor elements in pristine glass areas and corroded. The chemical results of the unaffected areas as indicated that the samples fall to the category of soda-lime-silica type (Table 6). The silica source of the assemblage is sand with natron as fluxing agent (Zacharias et al., 2008; Oikonomou, et al., 2012). The soda lime silica glasses are considered as highly resistant to corrosion mechanism (El-Shamy, 1973).

Table 6. EDS compositional bulk analysis of pristine glass areas in beads and vessels, mean values (weight %, normalised to 100%).

	SiO2	*Na2O*	*K2O*	*CaO*	*MgO*	*Al_2O_3*	*SO_3*	*Cl*
Beads	*72.75*	*13.15*	*0.44*	*8.17*	*0.5.37*	*1.6*	*0.46*	*1.16*
Vessels	*71.69*	*17.48*	*0.27*	*5.77*	*0.38*	*2.43*	*0.4*	*1.43*

The difference of the Na_2O on the pristine glass to the corroded was calculated. The mean percentage of the alkalis loss for glass beads was 71.48% and for vessels 93.37%. It was observed that the core formed vessels have a higher percentage of alkalis loss in comparison to glass beads. This variation is possible due to two purposes, the chemical composition and the manufacturing technique. The CaO considered to be a stabilizer and up to 10% reduces soda extraction. The CaO percentage of beads and vessels is 8.87% and 6.27% respectively. The vessels which have lower calcium concentrations are more likely to absorb water by the surface layers and corrode than the beads (Jackson, et al., 2012).

Corrosion patterns are present at the body of the vessels and at the decoration trails. Extensive pitting and iridescence are found in areas where the threads of different colored glass were wound around the glass body as it was expected. Observing a cross section SEM photography of sample Man 11, the lamination thickness at the edge of the white decoration trail is 5 times thicker than at the blue body (Fig. 9).

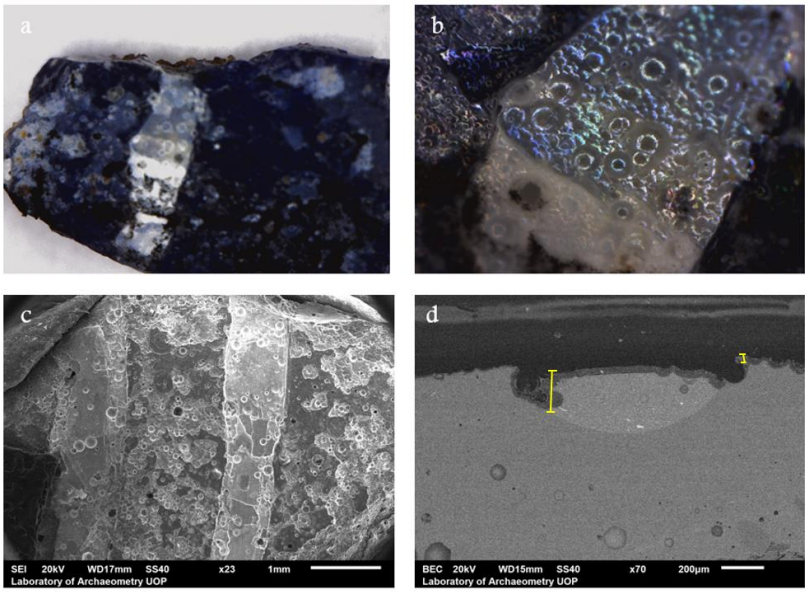

Figure 9. Sample Man 11: LED-OM Images a (up left) Iridescence (magnification x 50) and b (up left) iridescence and pitting (magnification x 200). SEM images c (down left) iridescence and pitting (magnification x 23) and d (down right) cross section of the sample. The lamination thickness appear to be 5-6 times thicker than at the blue body (magnification x 70).

To examine more thoroughly the vessels, depth profiling of SiO_2, CaO, Na_2O and Al_2O_3, was acquired from the cross-sections, in the approximate depth of 40 μm. It has resulted that in the blue areas occur lamination layers until 5 μm and the values of silica increase dramatically in this area in contrast to relatively low sodium values. At this area, a peak of aluminum was also observed and the values of calcium were increased in a very thin outer layer of the sample. An alumina- silica protective layer was formed, a typical type III corrosion surface formation (Hench & Clark, 1978). The extreme variations of the values of the examined elements stopped occurring near 8-10 μm deep from the surface (Fig. 10). To summarize, for the blue areas of the samples the corrosion depth determined around 6-8 μm, for the yellow areas were determined around 8-12 μm and for the white areas around 12-15 μm based on the concentrations of the alkalis mentioned before. The thickness of lamination at the edge of the decoration trails was clearly bigger than the blue body.

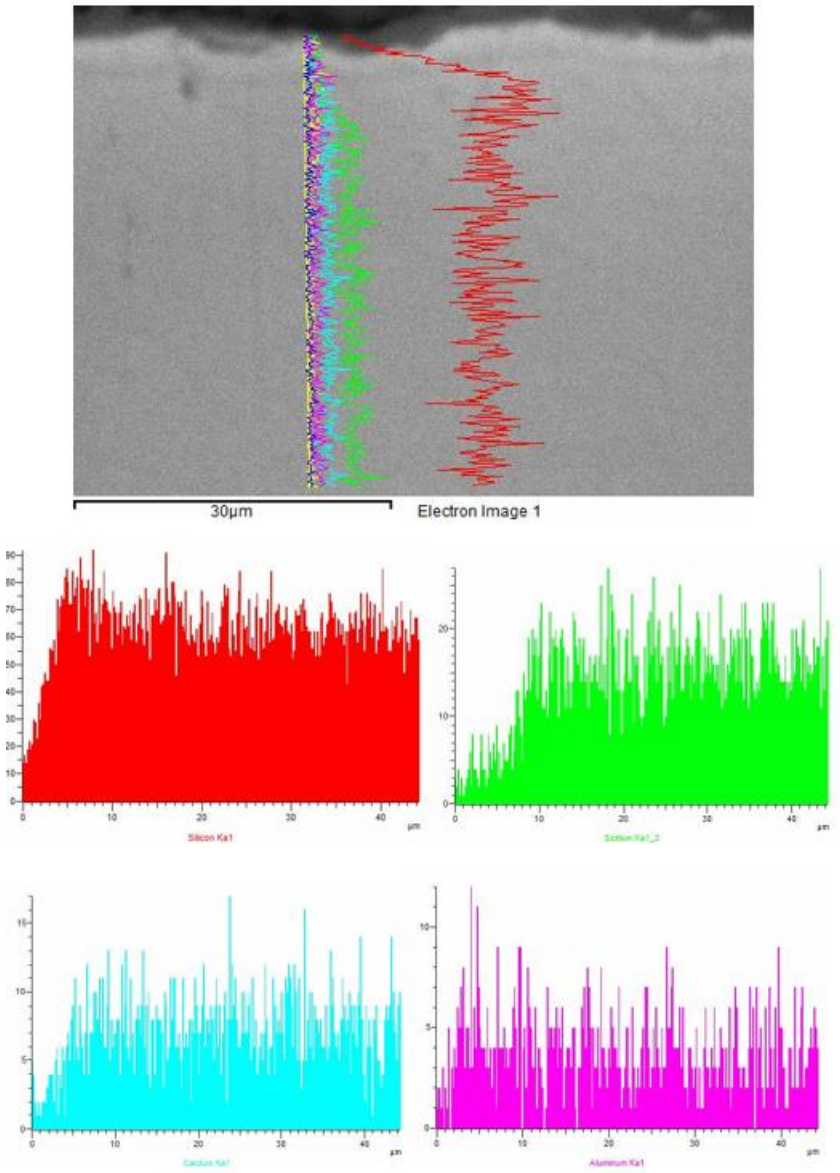

Figure 10. SEM-EDS Line Scanning Sample Man 7, core formed vessel, blue area. Graphs: red-silicon, green-sodium, aqua-calcium and violet-aluminum (0 µm: external surface)

As it was mentioned in previous sections, the main two corrosion factors are the composition and the environment the glass is exposed to. However, the surface modifications caused by different shaping technologies also influenced the rate and extent of glass surface degradation in this study. According to Hench and Clark (1978), the corrosion rate was accelerated logarithmically in glasses with a greater surface area. Experiments to ground glasses (Jackson, et al., 2012) showed that the alkalis loss was heavier in uneven surfaces. The lack of sleek surface increases and accelerate logarithmically the deterioration rate (Semenov et al. 1972). The core formed vessels and the two-colored beads endorse the hypothesis that surface unevenness accelerates the decay rate. When a glass appears to have an uneven surface, occurring valleys and the ridges, the exposure area to the corrosion factors is larger than to an even surface.

6. CONCLUSIONS

The present paper intends to add to the academic discussion regarding the complexity of glass corrosion mechanisms and products. More specifically, five case studies of buried archaeological glass are presented, aiming to further investigate the effect of the glass composition, the original content and the burial environment.

The examination of an assemblage of Ottoman glass from Kyparissia, Greece, highlights the effect of the glass composition on the mechanisms and degree of corrosion. Among the samples of the assemblage, the Na-rich glasses present the smallest degree of corrosion, with the formation of a silica-rich protec-

tive film, which is significantly depleted in alkalis, but the silica network is not damaged. K-rich glasses present stronger corrosion, with the formation of an external Al_2O_3-SiO_2 layer, which is not as effective in the protection of the core. Finally, the high-lead glasses present the thickest external layer of corrosion, with the significant depletion of K_2O.

In the Roman glass vessels for Patras, Greece, the effect of the original vessel content seems to play a significant role in the corrosion process. The inside surfaces of the sherds walls demonstrate high polymerization, a corrosion alteration not noted on the outside surfaces of the same samples. It is therefore suggested that the intense corrosion is due to the original content of the vessels, significantly affecting the glass over a short period.

For a Late Bronze Age beads from Ancient Methone, Pieria, additional to the observed loss of alkali and alkali earth components, the effect of microorganisms was examined through the presence of biocorrosion patterns (darkening of glass and presence of circular holes or groups of concentric circles). Finally, SO_3 was detected in the majority of the analysed beads but the study did not conclude weather its presence is due to the plant ash used or the action of microorganisms.

In the final case-study presented, that of an Archaic to Hellenistic assemblage of vase glass and glass beads from Thebes, a sophisticated profiling line-scan provided more evidence that the alkalis loss effects are clearly associated with the surface pattern and are more intense in areas of uneven geometry.

ACKNOWLEDGEMENTS

The authors acknowledge granted permits to study the material jointly given by the Ministry of Culture of Greece and the Archaeological Ephorates of Pieria, Achaia, Thebes and Messenia.

REFERENCES

Bertoncello, R., Milanese, L., Russo, U., Pedron, D., Guerriero, P. and Barison, S. (2002) Chemistry of cultural glasses: The early medieval glasses of Monselice's hill (Padova, Italy). *Journal of Non-Crystalline Solids*, Vol. 306, pp. 249-262.

Cagno, S., Nuyts, G., Bugani, S., De Vis, K., Schalm, O., Caen, J., Helfen, K., Cotte, M., Reischig, P. and Janssens, K. (2011) Evaluation of manganese-bodies removal in historical stained glass windows via SR-μ-XANES/XRF and SR-μ-CT. *Journal of Analytical Atomic Spectrometry*, Vol. 26, pp. 2442-2451.

Cox, G.A. and Ford, B.A. (1993) The long-term corrosion of glass by ground-water. *Journal of Materials Science,* Vol. 28, pp. 5637–5647.

Davison, S. (eds.) (2003) *Conservation and restoration of glass*. Oxford, Butterworth-Heinemann.

Doménech-Carbó, M.-T., Doménech-Carbó, A., Osete-Cortina, L. and Saurí-Peris, M.-C. (2006) A study on corrosion processes of archaeological glass from the Valencian region (Spain) and its consolidation treatment. *Microchimica Acta*, Vol. 154, pp. 123–142.

Dungworth, D., Cromwell, T., Ashurst, D., Cumberpatch, C., Higgins, D. and Willmott, H. (2006) Glass and pottery manufacture at Silkstone, Yorkshire. *Post-Medieval Archaeology,* 40/1, pp. 160-190.

Eastaugh, N., Walsh, V., Chaplin T. and Siddall, R. (eds.) (2004) The pigment Compendium, A dictionary of historical pigments. Oxford, Elsevier.

El-Shamy, T. M. (1973) The chemical durability of Na_2O–CaO–SiO_2 glasses, *Physics and Chemistry of Glasses*, Vol. 14, pp. 1-5.

Freestone, I. (2001) Post-depositional changes in archaeological ceramics and glasses. In: Brothwell, D.R., Pollard, A.M. (Eds.), Handbook of Archaeological Sciences Chichester, John Wiley, pp. 615–625.

Freestone, I. C., Ponting, M. and Hughes, M. J. (2002) The origins of Byzantine Glass from Maroni Petrera, Cyprus. *Archaeometry,* Vol. 44, No. 2, pp. 257–272.

Germanidou, S. and Gerolimou, K. (2015) The hamam of Kyparissia, western Messinia: An unknown Ottoman bath and its structure within the frame of local Ottoman architecture and topography, "Against Gravity - Bulding Practices in the Pre-Industrial World", Philadelphia, 20-22 March 2015, edited by R. Ousterhout, D. Borbonus and E. Dumser.

Harden, D.B. (1936) Roman Glass from Karanis found by the University of Michigan Archaeological Expedition in Egypt 1924–1929 (University of Michigan Studies, Humanistic Series, vol. xli). Ann Arbor, U.S.A., University of Michigan Press.

Hench, L.L. (1982) Glass surfaces. *Journal de Physique Colloques,* Vol. 43 (C9), pp. 625-636.

Hench, L.L. and Clark, D.E. (1978) Physical chemistry of glass surfaces. *Journal of Non-Crystalline Solids*, Vol. 28, pp. 83-105.

Hench, L.L., Clark, D.E. and Yen-Bower, E.L. (1980) Corrosion of glasses and glass-ceramics. N*uclear and Chemical Waste Management,* No. I, pp. 59-75.

Henderson, J. (2013) *Ancient glass: An interdisciplinary exploration*. New York: Cambridge University Press.

Jackson, C. M., Greenfield, D. and Howie, L. A. (2012) An assessment of compositional and morphological changes in model archaeological glasses in an acid burial matrix. *Archaeometry,* Vol. 54, No. 3, pp. 489–507.

Liritzis, I. (2020) Archaeometry: An overview. *Scientific Culture*, Vol. 6, No. 1, pp. 49-98.

Melcher, M. and Schreiner, M. (2013) Glass Degradation by Liquids and Atmospheric Agents. In: K. Janssens, ed., *Modern methods for analysing archaeological and historical glass*. Chichester, John Wiley and Sons Ltd, pp. 609-651.

Oikonomou, A. Beltsios, K. and Zacharias, N. (2012) Analytical and technological study of an ancient glass collection from Thebes, Greece: An overall assessment. Proceedings of the AIHV 18, D. Ignatiadou, A. Antonaras (eds.), Thessaloniki, pp. 75-80.

Palamara, E., Zacharias, N., Papakosta, L., Palles, D., Kamitsos, E.I. and Pérez-Arantegui, J. (2016) Studying a funerary Roman vessel glass collection from Patras, Greece: An interdisciplinary characterisation and use study. *STAR: Science & Technology of Archaeological Research*, Vol. 2, pp. 1–14.

Palamara, E., Zacharias, N., Germanidou, S. and Gerolymou, K. (2017) Analysis and Technology of Glass Finds from an Ottoman Bathhouse (hamam) in Kyparissia, Greece. *STAR: Science & Technology of Archaeological Research,* Vol 3, No. 2, pp. 376-390.

Perez y Jorba, M., Dallas, J.P., Bauer, C., Bahezre, C. and Martin, J.C. (1980) Deterioration of stained glass by atmospheric corrosion and micro-organisms. *Journal of Materials Science, Vol.* 15, pp. 1640–1647.

Polard, A.M. and Heron, C. (1996) Archaeological chemistry. Cambridge, The Royal Society of Chemistry.

Semenov, N. I. Paplauskas, A. B. and Ryabov, V. (1972) Effect of surface microstructure on the strength of glass. *Glass Technology*, 13 Vol.6, p. 171–5.

Rahman Nur Qahirah Abdul, Ramli, Z, Hussin, A, Nu'man Mohd Nasir, M, Nur Sarahah Mohd Supian, Dadian, H.S (2019) Elemental analysis by field-emission scanning electron microscope of ancient glass beads sample from pulau kalumpang archaeological site, (Perak, Malaysia), *Mediterranean Archaeology and Archaeometry*, Vol. 19, No 1, pp. 93-106. DOI: 10.5281/zenodo.2585992.

Schalm, O., Proost, K., De Vis, K., Cagno, S., Janssens, K., Mees, F., Jacobs, P. and Caen, J. (2011) Manganese staining of archaeological glass: The characterization on Mn-rich inclusions in leached layers and a hypothesis of its formation. *Archaeometry,* Vol. 53, No. 1, pp. 103-122.

Silvestri, A., Molin, G. and Salviulo, G. (2005) Archaeological glass alteration products in marine and land-based environments: Morphological, chemical and microtextural characterization. *Journal of Non-Crystalline Solids,* Vol. 351, pp. 1338-1349.

Tournié, A., Ricciardi, P. and Colomban, Ph. (2008) Glass corrosion mechanisms: A multiscale analysis. *Solid State Ionics*, Vol. 179, pp. 2142-2154.

Verney-Carron, Au. (2017) Studies on natural and archaeological glasses. Opportunities to learn about long-term nuclear waste glass corrosion. U.S. Nuclear Waste Technical Review Board. Available at http://www.nwtrb.gov/ [Accessed 17 September 2017].

Zacharias, N. Oikonomou, A. Beltsios, K. Karydas, A. Bassiakos, Y. Michael, C.T. Zarkadas, Ch (2008) Solid-State Luminescence Techniques Applied for the Examination of Archaeological Glass Beads, *Journal of Optical Materials*, Vol. 30, pp. 1127-1133.

Zacharias, N. and Palamara, E. (2016) Chapter 12: Glass Corrosion: Issues and Approaches for Archaeological Science in Recent Advances. In: *Scientific Research on Ancient Glass and Glasses*, Fuxi Gan, Qinghui Li and Julian Henderson (Eds.), World Scientific, pp. 233-248.